

Reduced Torque Ripple And Constant Torque Switching Frequency Strategy For Direct Torque Control Of Induction Machine

N.R.N. Idris and A.H.M. Yatim

Energy Conversion Dept.,
Universiti Teknologi Malaysia,
81310 UTM Skudai,
Johor, Malaysia

Tel: +607-550 5141 Fax: +607-556 6272
e-mail: nikrumzi@ieee.org

Abstract-The switching strategy of a conventional direct torque control (DTC) scheme which is based on hysteresis comparator results in a variable switching frequency which depends on the speed, flux, stator voltage and the hysteresis band of the comparator. This paper proposes a new switching strategy which compares the torque error from a PI controller with two triangular waveforms (180° phase shift) hence results in a constant torque switching frequency. Two triangular waveforms are necessary to ensure a four-quadrant operation of the DTC drive. The switching frequency of the DTC drive is determined by the frequency of the triangular waveforms and is almost independent from the speed. The simulation and experimental results are presented to validate this proposed scheme.

I. INTRODUCTION

More than a decade ago, direct torque control (DTC) was introduced to give a fast and good dynamic torque response and can be considered as an alternative to the field oriented control (FOC) technique [1,2]. The DTC scheme is very simple as shown by its basic configuration in Fig. 1; it consists of DTC controller, torque and flux calculator, and VSI. The configuration is much simpler than the FOC system due to the absence of frame transformer, pulse width modulator and position encoder, which introduce delays and requires mechanical transducer. The DTC controller comprises of selection table and hysteresis comparator, which are relatively easy to implement.

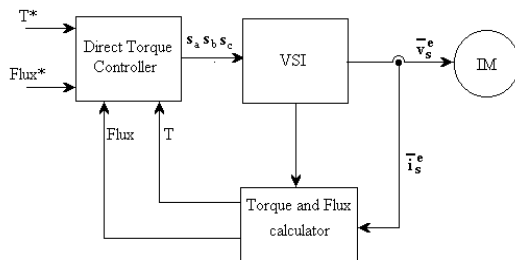


Fig. 1 Basic configuration of DTC

A DTC drive based on fixed torque hysteresis band, however, suffer from a varying rate of change of torque — which is simply referred to as torque slope — and hence torque controller switching frequency, as a function of motor speed, stator and rotor fluxes, and stator voltage; this in turn results in a varying device switching frequency. Variable switching frequency is undesirable since the switching capabilities of the inverter is not fully utilised [3,4,5]. For fixed torque band, the choice of the band's width is normally based on the worst condition which is limited by the thermal condition of the switching devices, thus operation for other condition is not optimised. This paper will discuss on a new torque controller which will result in a constant torque switching frequency and based on the fact that the switching frequency is mainly affected by the torque switching frequency [6,7], this will result in the former to be constant. Since it is necessary to fix the flux hysteresis band in order to control the THD of the phase current, the flux hysteresis band will be kept constant.

The rest of this paper is organised as follows. The effect of the torque and flux hysteresis bands on the performance of the DTC drive is given in section II. Section III presents the proposed torque controller and simulation results. Some experimental results are presented in section IV. Finally conclusion is given in section V.

II. EFFECT OF TORQUE AND FLUX HYSTERESIS BANDS ON THE DTC DRIVE PERFORMANCE

The performance of the hysteresis-based DTC drive which is affected by the hysteresis bands will be discussed based on the torque ripple, THD of the phase current and device switching frequency.

A. Torque Ripple

For precise position control application, particularly at low speed, it is necessary for the drive to produce a low electromagnetic torque ripple. As shown by [6], the torque ripple is only affected by the torque hysteresis band and is independent of the flux hysteresis band. It is also highlighted in [6] that the relation between the torque hysteresis band and

the torque dispersion is linear. Owing to the digital implementation, and the delay that exist between the instance the variables are sampled and the instance the voltage switching pattern is determined and pass to the inverter, there is an overshoot or undershoot in the electromagnetic torque above or below the torque hysteresis bands; this results in a non-zero ripple even a zero torque hysteresis band is applied. In three level torque hysteresis implementation, the width of the hysteresis torque band must be selected appropriately. If the band is too small, a torque overshoot which may cause the torque error to exceed the hysteresis band will occur [8,9]. This will result in a reverse voltage vector to be selected (instead of zero vector) to reduce the torque. A reverse voltage vector will reduce the torque rapidly and hence may in turn cause a torque undershoot. Therefore, the torque ripple can become high if the torque hysteresis band is set too small. Fig. 2. illustrate the scenario in which an overshoot in torque (undershoot in torque error) occurs which increases the torque ripple when the torque band is set too small.

B. THD of the phase current

In [6], a thorough investigation on the effect of torque and flux hysteresis bands on the performance of the DTC drive was carried out. It is shown that the flux hysteresis band strongly influences the total harmonic distortion (THD) of the phase current (as defined in the appendix). For a fixed torque hysteresis band, the THD increases with the flux hysteresis band. As the flux band is further increase, the flux locus approaches that of hexagonal shape, similar to that of the six-step inverter fed drive.

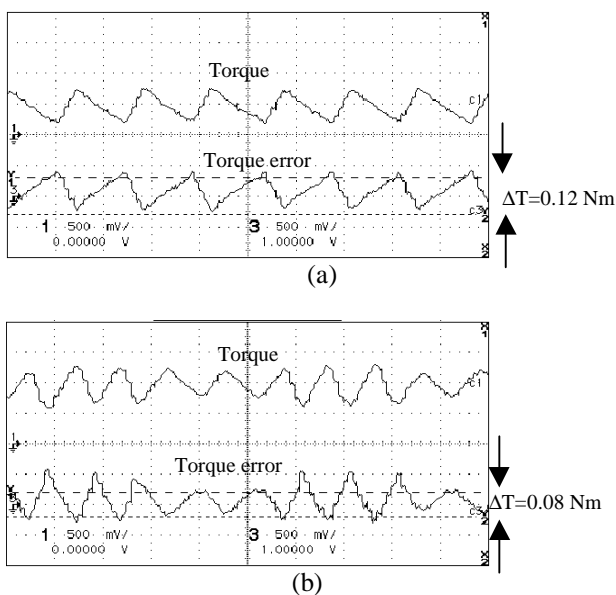


Fig. 2 Torque and torque error obtained from experimental results (a) Torque overshoot which does not exceed the hysteresis band, torque band = 0.12Nm (b) Torque overshoot which does exceed the hysteresis band, torque band = 0.08Nm

A simulation on the DTC drive is carried out with the torque hysteresis band varies from 5% to 25% of rated torque. The stator flux band is also varied from 2.5% to 15% of the command flux which is set to the rated value. The result is plotted as shown in Fig. 3 and it can be seen that the THD is mainly affected by the variation in stator flux hysteresis band than that of the torque hysteresis band.

C. Switching Frequency

It is shown in [6] that the switching frequency is mainly affected by the torque hysteresis band and increases with the width of the band. For a fixed torque band controller, it is therefore necessary to set the band to the maximum (or worst case) condition so that the switching frequency is guaranteed not to exceed its limit which is determined by the thermal restriction of the power devices [7].

Fig. 4 shows the 3-dimensional plot obtained from simulation showing the variation of the switching frequency (as defined in the appendix) with the flux and torque hysteresis bands, for three different rotor speeds. The figure indicates that the switching frequency is mainly affected by the width of the torque hysteresis band.

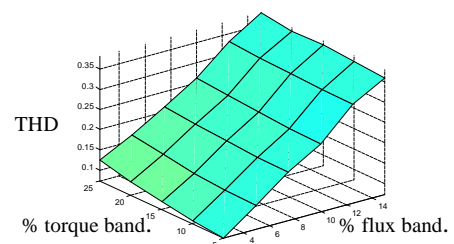


Fig. 3. Total harmonic distortion variation with stator flux and torque hysteresis bands

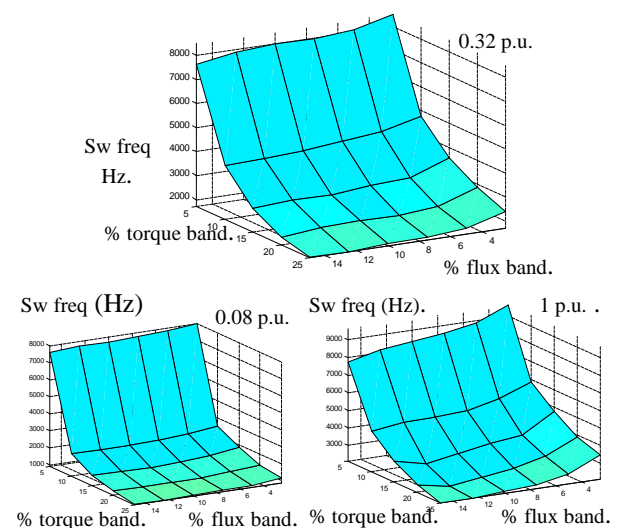


Fig. 4. Switching frequency variation with torque and flux hysteresis bands at 0.32 p.u., 0.08 p.u. and 1 p.u. of the rated rotor speed

In [10], it is highlighted that the torque slope is a function of motor speed, stator and rotor fluxes, and stator voltage. The equation of the torque slope for an increasing (slope^+) and decreasing (slope^-) torque at the sampling instant $(n+1)^{\text{th}}$ can be written as (1) and (2) respectively.

$$\text{slope}^+ \equiv \frac{T_{e,n+1} - T_{e,n}}{t_s} = -\frac{T_{e,n}}{\sigma\tau_{sr}} + \frac{3p}{4} \frac{L_m}{\sigma L_s L_r} [(\bar{v}_s - j\omega_r \bar{\psi}_s) \cdot j\bar{\psi}_r]$$

$$\text{slope}^- \equiv \frac{T_{e,n+1} - T_{e,n}}{t_s} = -\frac{T_{e,n}}{\sigma\tau_{sr}} + \frac{3p}{4} \frac{L_m}{\sigma L_s L_r} [(-j\omega_r \bar{\psi}_s) \cdot j\bar{\psi}_r]$$

Where, $1/(\sigma\tau_{sr}) = \frac{R_s}{\sigma L_s} + \frac{R_r}{\sigma L_r}$

and,

- R_s, R_r Stator and rotor resistance
- L_s, L_r Stator and rotor self inductance
- L_m Mutual inductance
- $\bar{\psi}_r, \bar{\psi}_s$ Rotor and stator flux linkages
- p Number of poles
- ω_r Rotor electrical angular velocity
- σ Total leakage factor
- t_s sampling period
- T_n estimated torque at n^{th} sampling instant

Since the torque slope varies with speed, the time taken for the torque to reach its upper and lower bands and consequently the torque switching frequency also varies with speed. The device switching frequency is directly affected by the torque switching frequency, therefore the former will vary with motor's speed. The average device switching frequency must also consider the portion contributed by the flux controller switching. However if the flux band amplitude is fixed at about 3.5% of its rated, the contribution of the flux controller to the variation in the switching frequency due to the variation in speed is relatively small when compared to the one contributed by the torque hysteresis controller switching [8]. Further, the variation is linearly related to the speed [5].

III. CONSTANT TORQUE SWITCHING COMPARATOR

The proposed torque controller consists of two triangular waveforms generators, a comparator and a PI controller as depicted in figure 4.1. The two triangular waves (which will be referred to as upper and lower carriers), are 180° out of phase. The dc offsets for upper and lower carriers are set to half of its peak-peak value; the upper dc offset is positive while the lower is negative.

In principle, the output of the proposed torque comparator is similar to that produced by the three level hysteresis comparator [1]. For a positive (counter-clockwise) rotation,

an active forward voltage is selected when the output of the controller, i.e. torque status, is 1. This happens when the PI

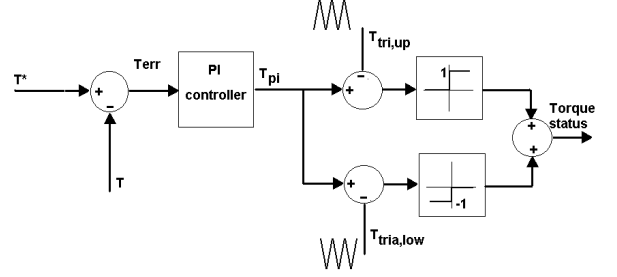


Fig 5. Proposed torque controller

controller output signal, T_{pi} , is larger than the upper carrier. A zero voltage vector (which will reduce the torque) is selected when torque status is 0. When a sudden reduction in torque is applied such that T_{pi} falls below the lower carrier, the torque status becomes -1 hence a reverse voltage vector will be selected; the drive will be operating in the fourth quadrant region. For a clockwise mechanical speed, the torque status is -1 for an active clockwise voltage vectors and again 0 for a zero voltage vectors. Operation will be in the third quadrant region and the re-generative braking mode of operation in the second quadrant region.

To study the performance of the proposed torque controller, a closed-loop speed control of the DTC drive is simulated using Matlab/Simulink simulation package. To imitate an actual digital implementation, the sampling rate is set to $60\mu\text{s}$ and a feedback delay of $40\mu\text{s}$ is added.

A. Torque ripple

In the proposed torque comparator, the undesired reverse voltage will be selected if the output of the PI controller falls below the lower carrier. The possibility that this happening increases as the slope of the signal is larger than that of the carrier. This is particularly true at low speed where the absolute value of slope for the increasing torque is larger than the slope of the decreasing torque. To limit the slope, the proportional gain of the PI controller has to be limited..

To illustrate this, the DTC drive is simulated with the proportional gain of the proposed torque controller set to give a steep negative slope such that it falls below the lower carrier hence resulting in a reverse voltage vector selection. The upper trace of Fig 6 shows the torque status, which is a three level output, used to select appropriate voltage vectors. A forward, zero and reverse voltage vectors will be selected corresponding to the positive, zero and negative torque status respectively. The lower trace shows the carrier waves ($T_{\text{tria,up}}$ and $T_{\text{tria,low}}$) and the PI controller output (T_{pi}). The large controller gain which results in a steep slope and hence causing the signal to fall below the lower carrier. The occurrence of the negative torque status can be reduced by reducing the proportional gain which on the other hand is constrained by the steady state torque error. Fig. 7 shows the

waveforms with the proportional gain reduced which clearly illustrate the elimination of the -1 torque status.

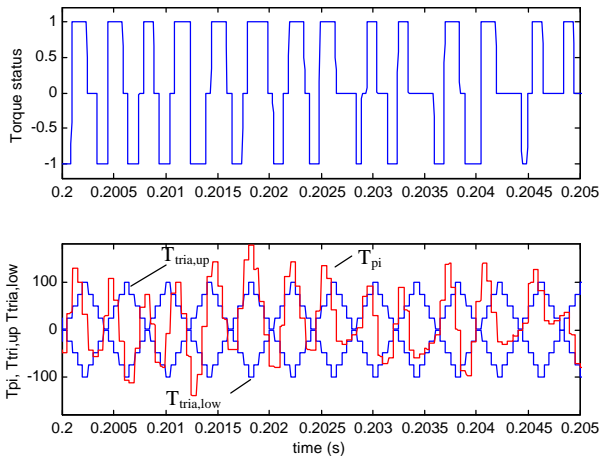


Fig. 6. The generation of the torque status based on the comparison between the carriers and the PI controller output with a large proportional gain

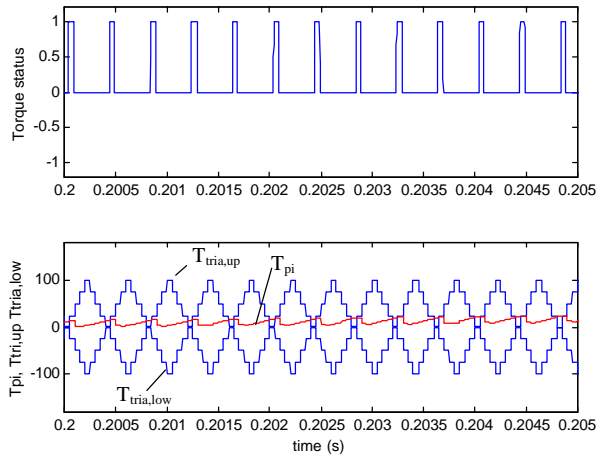


Fig. 7. The generation of the torque status based on the comparison between the carriers and the PI controller output with an appropriate proportional gain

The comparison of the torque ripple between a low and high gain of the controller as well as hysteresis-based controller is depicted in Fig 8. The hysteresis torque band amplitude is set to 5%, but owing to the $40\mu\text{s}$ delay, a reverse voltage vector is still selected.

B. Total harmonic distortion

As stated earlier on, to ensure a control over the THD of the phase current, the stator flux hysteresis band is fixed for this particular case to 0.07 p.u. Fig 9 shows the simulated phase current of IM, line-line voltage and frequency spectrum of the hysteresis-based torque and the proposed controllers, with the speed reference set to 50 rad/s. The phase current waveforms and its associated frequency spectrum indicate

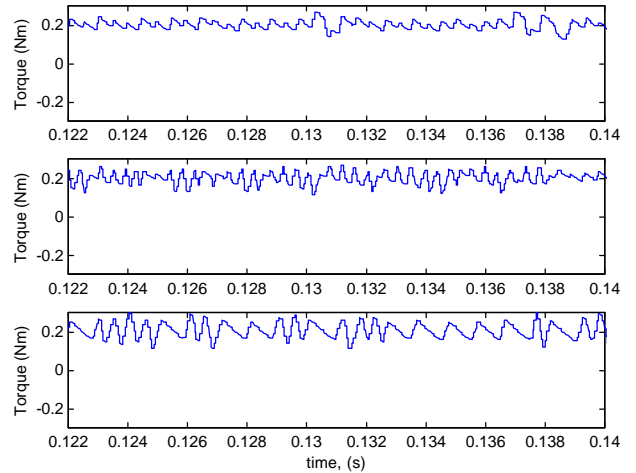


Fig. 8. Comparison between the proposed torque controller. Top trace: gain set appropriately, middle trace: gain set too high, bottom trace: hysteresis-based controller.

that the two controllers produces the same content of low harmonic current distortion. In other words, the proposed controller does not affect the THD or the low harmonic contents of the phase current. Due to the undesired reverse voltage vector selected, the line-line voltage for the hysteresis-based controller is no longer optimised.

C. Switching frequency

The average switching frequency of the simulated DTC drive with the proposed controller and the hysteresis-based controllers are calculated for four different speed setting. The width of the torque hysteresis band is set to 10% while the frequency of the carrier for the proposed controller is set to 2 kHz. The results as given in Table 1, shows that the proposed controller has managed to maintain the switching frequency around the carrier frequency regardless of the rotor speed.

TABLE I

SWITCHING FREQUENCY AT DIFFERENT ROTOR SPEED

Rotor speed (p.u.)	Switching frequency (kHz)	
	Proposed controller	Hysteresis-based controller
0.24	2.04	2.21
0.48	2.14	3.60
0.73	2.29	4.38
1	2.32	4.14

IV. EXPERIMENTAL RESULTS

The proposed torque controller was experimentally evaluated using the set-up shown in Fig. 10. The set-up consists of a

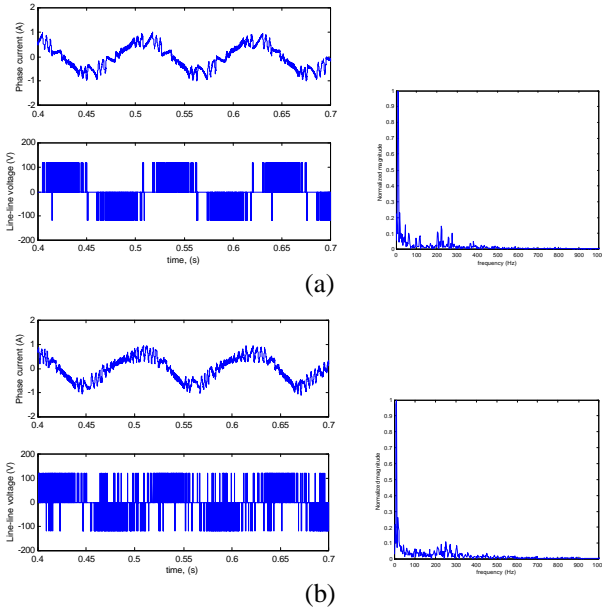


Fig. 9. Phase current, line-line voltage and low frequency spectrum of the phase current. (a) proposed torque controller. (b) hysteresis-based controller

3-phase IGBT inverter and a standard 2-pole, $\frac{1}{4}$ HP induction machine. All of the DTC control functions including the proposed torque controller and the closed-loop speed control functions are performed by the TMS320C31 DSP contained on the DS1102 controller board from dSPACE. The sampling period used for all the test is 60 μ s. The blanking time and selection table are implemented using the Xilinx XC4005E FPGA. The stator flux is estimated using the voltage model-based estimation technique with some low pass filtering [12]. The speed, which is obtained from the low-resolution encoder – 200 p.p.r. – is used only for the speed control system purposes.

Based on the simulation results, the drive is found to be performing satisfactorily when the proportional gain of the controller is set to 1500. The waveform of carrier, the output of the PI controller and the torque status for this gain setting is shown in Fig 12. Fig. 13 shows the waveforms when the gain is set too high (i.e. 2200) ; causing the undesired selection of the reverse voltage vector to reduce the torque. Fig 11 and 12 conform with the simulation results shown in Fig 6 and 7.

Fig. 13(a)-(c) shows the estimated electromagnetic torque of the DTC drive running at a constant speed of 10 rad/s. The top trace of Fig.13(a)-(c) is the torque status while the bottom trace shows the electromagnetic torque. Fig. 13(a) shows the torque with the correct setting of the proportional gain while that of Fig 13(b) is when the gain is set too high. Fig 13(c) shows the torque response for the hysteresis-based controller. Clearly, the top trace exhibits the minimum torque ripple as previously obtained from the simulation results of Fig. 8.

The frequency spectrum of the phase current for rotor speed of 10 rad/s, 30 rad/s and 60 rad/s with the proposed

torque controller and the hysteresis-based controller (torque band set to 0.04Nm) is shown in Fig.14 (obtained from an oscilloscope). Due to the constant torque switching frequency, the harmonic component of the phase current is concentrated around the carrier frequency and its multiple, rather than widely distributed as obtained for the hysteresis-based controller. For this particular set-up, carrier frequency is set to 2.5 kHz

To look at the dynamics of the proposed controller, a square wave speed command is applied and the waveforms of the rotor speed, torque and d-axis stator flux is as shown in Fig. 15. For comparison, the same command is applied to the hysteresis-based torque controller with the results shown in Fig. 16. With the proposed controller, the dynamic performance of the DTC drive is not impaired.

V. CONCLUSION

A new torque controller which produces constant torque switching frequency has been presented. The importance of proportional gain selection for the controller has been highlighted. Simulation results on the DTC drive showed that the proposed controller has managed to reduce the torque ripple, and maintained the switching frequency around the carrier frequency. By making the stator flux hysteresis band constant, it was shown that the low frequency harmonic of the phase current can be maintained. The proposed controller has also shown to give good dynamic torque response. Results from experiment carried out were in close agreement with the theoretical and simulation works.

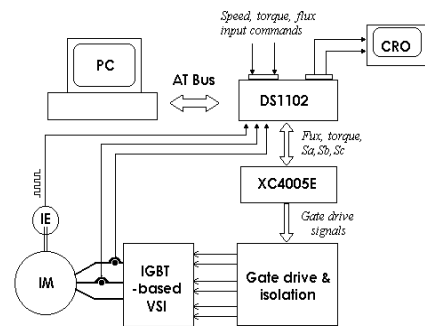


Fig. 10. Experimental set-up

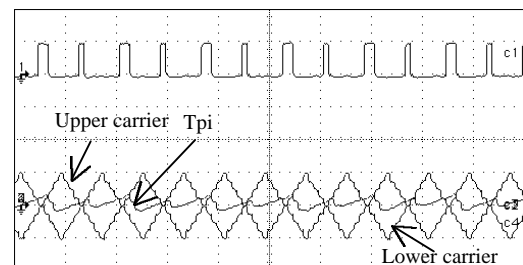


Fig 11 Torque status pattern generation for the proposed controller. Top trace: torque status, bottom trace: upper and lower carrier, and the output of the PI controller.

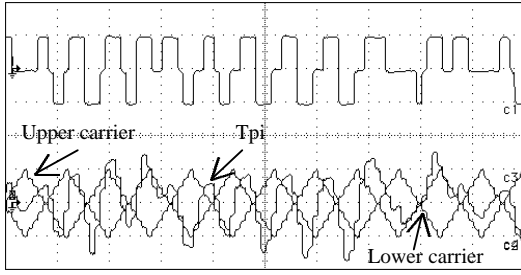
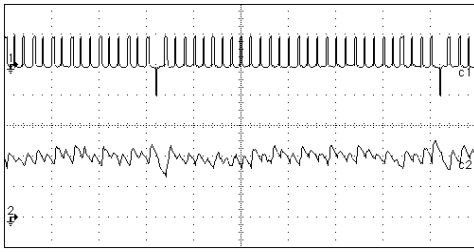
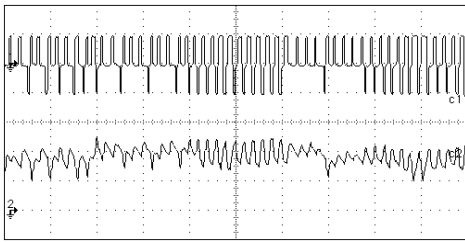


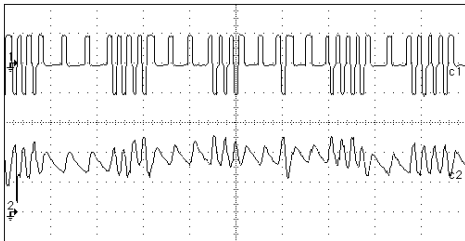
Fig 12. Torque status pattern generation for the proposed controller with the gain set too high. Top trace: torque status, bottom trace: upper and lower carrier, and the output of the PI controller (100 Nm/div).



(a)

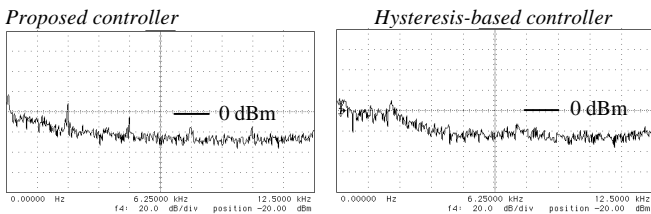


(b)

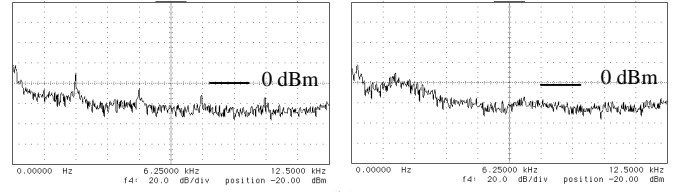


(c)

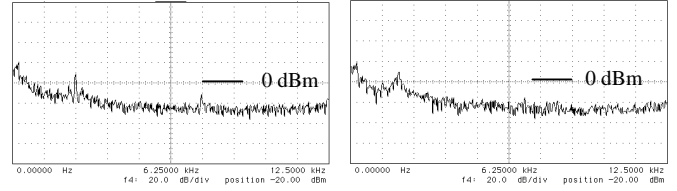
Fig. 13. Torque status and torque (0.1 Nm/div). (a) proposed controller – appropriate gain. (b) proposed controller – gain to high. (c) hysteresis-based controller



(a)



(b)



(c)

Fig. 14. Frequency spectrum of the phase current at rotor speed of (a) 10 rad/s, (b) 30 rad/s, and (c) 60 rad/s. Horizontal: 1.25kHz/div, vertical: 20dBm/div

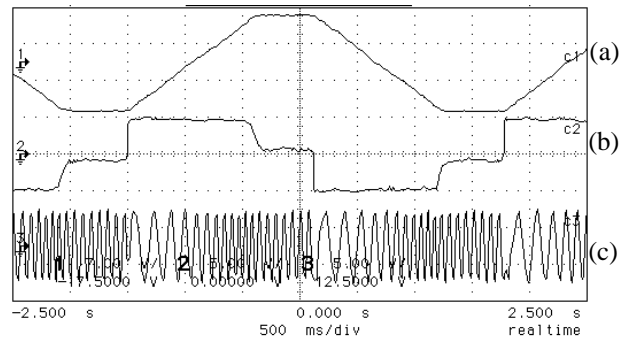


Fig. 15. Response for a square wave speed reference for the proposed torque controller (a) Rotor speed ($63 \text{ rad/s}^{-1}/\text{div}$). (b) Torque (1 Nm/div). (c) d-axis stator flux (0.5 Wb/div)

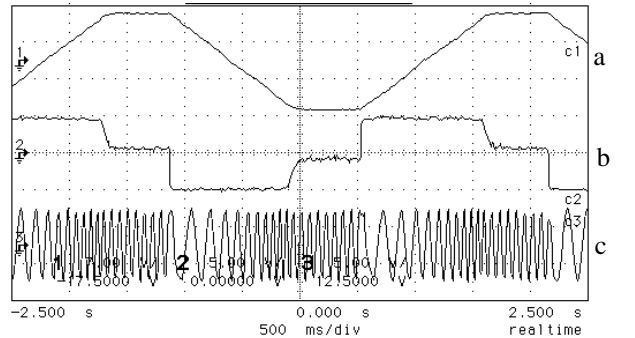


Fig. 16. Response for a square wave speed reference for a hysteresis-based controller (a) Rotor speed ($63 \text{ rad/s}^{-1}/\text{div}$). (b) Torque (1 Nm/div). (c) d-axis stator flux (0.5 Wb/div)

APPENDIX

A. Motor parameters used for the simulation and experimental

$$\begin{aligned} R_s &= 10.9 \, \Omega & R_r &= 9.25 \, \Omega & L_r &= 0.858792 \, \text{H} \\ L_s &= 0.858792 \, \text{H} & L_m &= 0.828981 \, \text{H} \end{aligned}$$

B. Definition of Switching frequency (f_{sw}) and Total Harmonic Distortion (THD)

$$f_{sw} = N_s / T_f$$

where,

N_s = Number of switching in one fundamental period

T_f = Fundamental period

$$THD = \sqrt{\frac{(I^2 - I_1^2)}{I_1^2}}$$

where,

I = rms value of the phase motor current.

I_1 = rms value of the fundamental harmonic component of the phase motor current.

REFERENCES

- [1] I.Takahashi, T. Noguchi, "A new quick-response and high-efficiency control strategy of an induction motor", *IEEE Trans. Ind. Appl.*, vol IA-22, No 5 Sept/Oct 1986
- [2] P.Tiitinen, "The next generation motor control method, DTC direct torque control", *Proceeding of Int. Conf on Power Electronics, Drives and Energy System for industrial growth*, N.Delhi, India, 8-11 Jan., 1996
- [3] J. Holtz, "Pulsewidth Modulation for the Electronic Power Conversion", *Proceeding of the IEEE*, Vol. 82, No. 8, Aug. 1994
- [4] B.K. Bose, "An adaptive hysteresis-based current control system", *IEEE Trans. Ind. Electron.*, Vol. 37, No. 5, Oct. 1990
- [5] J.K. Kang, D.W. Chung and S.K. Sul, "Direct torque control of induction machine with variable amplitude control of flux and torque hysteresis bands", in *Conf. Rec. IEEE-IAS*, 1999
- [6] D. Casadei, G. Grandi, G. Serra, A. Tani, "Effect of flux and torque hysteresis band amplitude in direct torque control of induction motor", *IECON '94*, Bologna, Italy, 5-9 Sept 1994
- [7] A. Monti, F.Pironi, F. Sartogo and P. Vas, "A new state observer for sensorless DTC control", *Power electronics and variable speed drives*, 21-23 Sept. 1998
- [8] T. Naguchi and I. Takahashi, "High frequency switching operation of PWM inverter for direct torque control of induction motor", in *Conf. Rec. IEEE-IAS*, pp775-780, 1997.
- [9] I.G. Bird and H. Zaleya, "Fuzzy logic torque ripple reduction for DTC based AC drives", *Electronics letters*, Vol. 33, No. 17, 14th Aug., 1997
- [10] J.K. Kang and S.K. Sul, "Torque ripple minimization strategy for direct torque control of induction motor", in *Conf. Rec. IEEE-IAS*, pp438-443, 1998
- [11] M.P. Kazmierkowski and A.B. Kasprowicz, "Improved direct torque and flux control of PWM inverter-fed induction motor drives", *IEEE Trans. Ind. Electronics*, Vol. 42, No. 4 Aug 1995
- [12] K.D. Husrt, T. G. Habetler, G. Griva, F. Profumo, "Zero speed tacholeless IM torque control: Simply a matter of stator voltage integration", *IEEE Trans Ind Appl.*, vol 34, no. 4, July/August 1998